Detailed Chemical Kinetics Model for Supercritical Water Oxidation of C_1 Compounds and H_2

Eric E. Brock and Phillip E. Savage
Dept. of Chemical Engineering, The University of Michigan, Ann Arbor, MI 48109

A detailed chemical kinetics model comprising 148 reversible elementary reactions for the supercritical water oxidation (SCWO) of methane, methanol, carbon monoxide and hydrogen was developed. Rate constants were taken from previous critical evaluations. The Lindemann model, at times modified with a broadening parameter, was used to account for the effects of pressure on the kinetics of unimolecular reactions. Model predictions were compared with published experimental SCWO kinetics data for $450-650°C$ and $240-250$ atm. The model correctly predicted global reaction orders for all four fuels to within their uncertainties. In addition, the model correctly predicted that the global reaction orders for O_2 during methanol and hydrogen oxidation were essentially zero, and that the O_2 concentration had the greatest effect on the methane oxidation rate. The pseudo-first-order rate constants predicted by the model were consistently higher than the experimental values, but the global activation energies were predicted correctly for methane oxidation and for CO and H_2 oxidation at high temperatures. The model's predictions generally became worse as the temperature decreased toward the critical point of water. A sensitivity analysis revealed that fewer than 20 elementary reactions largely controlled the oxidation kinetics for the compounds studied. Nearly half of these reactions involved HO_2, which is an important free radical for SCWO. Quantitative agreement with the experimental methane conversions was obtained by adjusting the preexponential factors for three elementary reactions within their uncertainties. It could also be obtained by using the JANAF value (0.5 kcal/mol) for the standard heat of formation of HO_2, but this value is lower than other recently recommended values.

Introduction

Supercritical water oxidation (SCWO) is an efficient technology for the complete oxidative destruction of organic compounds in water. The process operates at temperatures and pressures that exceed the critical point of water (374°C, 218 atm). At supercritical reaction conditions organic compounds (Connolly, 1966), gases (Pray et al., 1952), and water form a single homogeneous phase. The presence of a single phase and high temperatures allows the oxidation reactions to proceed rapidly, unhindered by interphase mass transfer.

SCWO has several advantages over the more established waste treatment methods of incineration and wet-air oxidation (Modell, 1989). SCWO can rapidly and completely oxidize a large variety of compounds. This feature reduces the possibility of products of incomplete combustion being released to the environment. The SCWO process can be quickly bottled up and the reactor effluent recycled back to the reactor should a system upset occur. The reactor and associated equipment can also be made sufficiently small that it could be transported to waste sites, removing the need to transport hazardous materials over long distances.

The advantages offered by SCWO have led to increasing interest in the chemistry and kinetics of SCWO because knowledge of the reaction kinetics is required to design, optimize, control, and analyze the SCWO process. Initial research, which focused on technology demonstration, provided the destruction efficiency of SCWO at various temperatures for a wide range of compounds (Modell, 1989; Thomason and Modell, 1984). These studies demonstrated the feasibility of SCWO, but they provided little understanding of the fundamental chemistry and kinetics. Further studies have focused

on the development of empirical global rate laws for the oxidation of representative organic pollutants (Crain et al., 1993; Gopalan and Savage, 1994; Li et al., 1992, 1993; Savage and Smith, 1994; Thornton and Savage, 1992a,b; Lee and Gloyna, 1992; Yang and Eckert, 1988). The utility of global reaction rate laws is limited, however. They can only be extrapolated to conditions other than those investigated experimentally with uncertainty. They will fail to account for any interactions that may occur during the treatment of mixtures of different compounds. Moreover, an approach that relies exclusively on extensive experimental studies with individual compounds is time-consuming and expensive when one considers the large number of individual compounds and mixtures that SCWO can treat. Clearly, a more general and efficient approach for modeling SCWO kinetics and pathways is desirable.

Detailed chemical kinetics models, which are based upon the governing reaction mechanism, provide just such an approach. These models use the elementary reaction steps and their associated kinetics to describe quantitatively the behavior of the reacting system. After such a model has been validated by comparing its predictions with experimental data, the model can be used to investigate the effects of important process variables such as temperature, pressure, and reactant concentrations. Using an accurate detailed chemical kinetics model can provide information in a fraction of the time required to run similar experiments. Such a model would possess engineering utility, and it could be used to optimize the design of a commercial SCWO reactor. An optimal design could be one that achieves a specific destruction efficiency at the minimum residence time and temperature or one that minimizes the concentration of undesired byproducts that may be more hazardous than the original reactants (Thornton et al., 1991).

The literature currently provides detailed chemical kinetics models for the oxidation of CH_4, CH_3OH, CO, and H_2 (Holgate and Tester, 1993, 1994b; Rofer and Streit, 1988, 1989; Webley et al., 1990; Webley and Tester, 1991). These models have met with different degrees of success in reproducing experimental data. Webley and Tester (1991) developed a model for the SCWO of methane. This model underpredicted the rate of oxidation, and it also predicted an activation energy that was much higher than that determined experimentally. Rofer and Streit (1988) developed a model for CH_4, CH_3OH, and CO. This model described SCWO of methane reasonably well, but it overpredicted the pseudo-first-order rate constant for methanol by approximately an order of magnitude, and it predicted the wrong activation energy for CO oxidation. These authors noted that their model gave the most accurate predictions at the higher temperatures (> 770 K). Holgate and Tester's (1994b) recent model for CO oxidation does an excellent job of predicting the CO oxidation rate for fuel-rich mixtures at high temperatures. The authors noted, however, that fuel-lean mixtures and reactions at low temperatures were not modeled accurately. Holgate and Tester's (1993) model for H_2 oxidation gave good predictions of the observed kinetics, but the authors noted that this result might have been the fortuitous combination of inaccuracies in the predicted induction times and kinetic decay constants. We note too that the recent models for H_2 and CO used a value for the heat of formation of HO_2 that is lower

than the values recently recommended. The authors acknowledge this, but found that the value they used allowed their models to match experimental observations much better.

Cochran et al. (1992) took the shortcomings of some of the earlier detailed chemical kinetics models to imply that such pressure-corrected combustion models could not adequately describe SCWO kinetics. They suggested that molecular-level simulations were required to understand and model the rate processes properly.

This article describes a new and unified detailed chemical kinetics model for the oxidation of simple H–C–O compounds in supercritical water (SCW). We focus exclusively on the disappearance kinetics for such simple compounds. The mechanism includes more steps than previous models for this system, and it uses more recent thermodynamic and kinetic data. The model accounts for the effects of pressure on all unimolecular reactions and some chemically activated bimolecular reactions. Broadening parameters are also used for the reactions for which data were available. This is the first time that a single detailed chemical kinetics model has been constructed to describe the SCWO of CH_4, CH_3OH, CO, and H_2.

Model Development

The present detailed chemical kinetics model is based on a mechanism that comprises 22 species and 148 elementary, reversible, free-radical reactions. We excluded ionic reactions from the mechanism because the water density, and hence K_w, are sufficiently low that ionic reactions should not be competitive under the conditions being modeled (450–650°C, 240–250 atm) (Antal et al., 1987). For example, at 500°C and 250 bar, K_w is about eight orders of magnitude lower than it is in ambient liquid water (Marshall and Franck, 1981). The elementary reactions that make up the mechanism were developed by identifying 22 different radicals or molecules that contain no more than one carbon atom and oxygen and hydrogen, and then initially considering essentially all possible reactions between these 22 different species. The atmospheric chemistry and combustion literature provided valuable guidance. Rate parameters, which include a preexponential factor, a temperature exponent, and an energy of activation were taken from recent critical reviews of kinetic data when available (Baulch et al., 1992; Tsang, 1987; Tsang and Hampson, 1986; Warnatz, 1984). We estimated parameters for a few reactions for which the literature provided no data. The bases for these estimates will be explained later. Table 1 lists the elementary reactions and their reaction rate parameters. Some of the reactions listed in the table have low rates at the temperatures investigated to date. Nevertheless, the slow reactions have been retained in the present model for completeness. It is conceivable that such reactions could become important at different reaction conditions.

This set of elementary reactions and the initial concentrations of the reactants allow one to model the reacting system as a set of 22 differential equations that describes the change in the concentration of each compound with residence time in an isothermal, plug-flow reactor. Equation 1 illustrates the form that one of these differential equations would take:

Table 1. SCWO Mechanism with Kinetic Parameters

	Reactions[a]	A^b	n	E_a^c
1	$CH_4 + H = CH_3 + H_2$	1.33E+04	3.00	$8,038^d$
2	$CH_4 + O_2 = CH_3 + HO_2$	3.97E+13	0.00	$56,894^d$
3	$CH_4 + O = CH_3 + OH$	6.92E+08	1.56	$8,485^d$
4	$CH_4 + OH = CH_3 + H_2O$	1.57E+07	1.83	$2,782^d$
5	$CH_4 + HO_2 = H_2O_2 + CH_3$	9.04E+12	0.00	$24,641^d$
6	$CH_4 + CH_3O = CH_3OH + CH_3$	1.57E+11	0.00	$8,843^e$
7	$CH_4 + CH_2 = CH_3 + CH_3$	4.30E+12	0.00	$10,039^f$
8	$CH_4 + CH_2OH = CH_3OH + CH_3$	2.16E+01	3.10	$16,227^g$
9	$CH_4 + HCO = CH_2O + CH_3$	7.27E+03	2.85	$22,515^e$
10	$CH_4 + CH_3O_2 = CH_3O_2H + CH_3$	1.81E+11	0.00	$18,481^e$
11	$CH_4(+M) = CH_3 + H(+M)$	3.71E+17	−0.558	$104,888^{hh}$
		LOW/1.29E+33	−3.732	$106,506/^{hh}$
		SRI/0.45	797	$7,791/^{hh}$
		K_c 14.6	0.26	$104,572^{hh,ii}$
12	$CH_3 + H = CH_2 + H_2$	6.03E+13	0.00	$15,103^d$
13	$CH_3 + O_2 = CH_3O + O$	1.32E+14	0.00	$31,398^d$
14	$CH_3 + O_2(+M) = CH_3O_2(+M)$	7.83E+08	1.20	0^d
		LOW/5.81E+25	−3.30	$0/^d$
		TROE/$F_c = 0.466 − 1.30 \times 10^{-4}T/^d$		
15	$CH_3 + O_2 = CH_2O + OH$	3.31E+11	0.00	$8,942^d$
16	$CH_3 + O = CH_3O$	7.95E+15	−2.12	624^h
17	$CH_3 + O = H + CH_2O$	8.43E+13	0.00	0^d
18	$CH_3 + O = CH_2 + OH$	5.00E+13	0.00	$1,200^i$
19	$CH_3 + OH = CH_3O + H$	5.74E+12	−0.23	$13,930^h$
20	$CH_3 + OH = CH_2O + H_2$	3.19E+12	−0.53	$10,810^h$
21	$CH_3 + HO_2 = CH_3O + OH$	1.81E+13	0.00	0^d
22	$CH_3 + CH_3O = CH_4 + CH_2O$	2.41E+13	0.00	0^e
23	$CH_3 + CH_2OH = CH_4 + CH_2O$	2.41E+12	0.00	0^g
24	$CH_3 + HCO = CH_4 + CO$	1.21E+14	0.00	0^e
25	$CH_3 + CH_3O_2 = CH_3O + CH_3O$	2.41E+13	0.00	0^e
26	$CH_3(+M) = CH_2 + H(+M)$	3.16E+15	0.00	$109,720^{bb}$
		LOW/1.02E+16	0.00	$90,616/^d$
27	$CH_3O + H = CH_2O + H_2$	1.81E+13	0.00	0^d
28	$CH_3O + O_2 = CH_2O + HO_2$	3.61E+10	0.00	$2,126^d$
29	$CH_3O + O = CH_2O + OH$	6.03E+12	0.00	0^e
30	$CH_3O + OH = CH_2O + H_2O$	1.81E+13	0.00	0^e
31	$CH_3O + HO_2 = CH_2O + H_2O_2$	3.01E+11	0.00	0^e
32	$CH_3O + CH_3O = CH_2O + CH_3OH$	6.03E+13	0.00	0^e
33	$CH_3O + CH_3OH = CH_3OH + CH_2OH$	3.01E+11	0.00	$4,074^g$
34	$CH_3O + CH_2 = CH_3 + CH_2O$	1.81E+13	0.00	0^e
35	$CH_3O + CH_2O = CH_3OH + HCO$	1.02E+11	0.00	$2,981^e$
36	$CH_3O + CH_2OH = CH_3OH + CH_2O$	2.41E+13	0.00	0^g
37	$CH_3O + HCO = CH_3OH + CO$	9.04E+13	0.00	0^e
38	$CH_3O + CO = CH_3 + CO_2$	1.57E+13	0.00	$11,804^e$
39	$CH_3O + CH_3O_2 = CH_2O + CH_3O_2H$	3.01E+11	0.00	0^e
40	$CH_3O(+M) = CH_2O + H(+M)$	1.60E+14	0.00	$25,096^k$
		LOW/1.90E+26	−2.70	$30,603/^d$

$$\frac{d[CH_4]}{d\tau} = -k_1[CH_4][H] - k_2[CH_4][O_2] -$$
$$\dots + k_{-1}[CH_3][H_2] + \dots \quad (1)$$

where k_1, k_2, and k_{-1} are the rate constants for reaction 1, reaction 2, and the reverse of reaction 1, respectively. The set of equations was solved numerically using the CHEMKIN II package developed at Sandia National Laboratories (Kee et al., 1990, 1991). This package of FORTRAN programs solves systems of stiff differential equations that describe homogeneous gas-phase reactions.

Thermodynamics

The CHEMKIN package also includes thermodynamic data for many gas-phase species common to combustion systems.

This information was used to calculate thermodynamically consistent reverse reaction rate constants. Reverse reaction rate constants, k_r, can be calculated from the equilibrium constant, K_c, and the forward rate constant, k_f, by

$$k_r = \frac{k_f}{K_c} \quad (2)$$

K_c is related to K_p by

$$K_c = \frac{K_p}{K_\phi} \left(\frac{P_{atm}}{ZRT} \right)^{\Sigma \nu_i} \quad (3)$$

where K_p, the partial-pressure-based equilibrium constant, can be calculated from tabulated free energies of formation;

Table 1(continued). SCWO Mechanism with Kinetic Parameters

	Reactions[a]	A[b]	n	E_a^c
41	$CH_3OH + H = CH_3O + H_2$	4.00E+13	0.00	$6,095^k$
42	$CH_3OH + H = H_2 + CH_2OH$	8.18E+13	0.00	$7,592^l$
43	$CH_3OH + H = CH_3 + H_2O$	1.00E+13	0.00	$5,300^l$
44	$CH_3OH + O_2 = CH_2OH + HO_2$	2.05E+13	0.00	$44,911^g$
45	$CH_3OH + O = OH + CH_2OH$	1.72E+13	0.00	$4,914^m$
46	$CH_3OH + O = OH + CH_3O$	1.00E+13	0.00	$4,684^k$
47	$CH_3OH + OH = H_2O + CH_2OH$	1.35E+13	0.00	$1,881^l$
48	$CH_3OH + OH = H_2O + CH_3O$	1.00E+13	0.00	$1,697^k$
49	$CH_3OH + HO_2 = H_2O_2 + CH_2OH$	9.64E+10	0.00	$12,579^g$
50	$CH_3OH + CH_2 = CH_3 + CH_2OH$	3.19E+01	3.20	$7,172^g$
51	$CH_3OH + CH_2 = CH_3 + CH_3O$	1.44E+01	3.10	$6,935^g$
52	$CH_3OH + HCO = CH_2O + CH_2OH$	9.66E+03	2.90	$13,108^g$
53	$CH_3OH + CH_3O_2 = CH_3O_2H + CH_2OH$	1.81E+12	0.00	$13,712^g$
54	$CH_3OH(+M) = CH_2OH + H(+M)$	3.16E+15	0.00	$96,010^{bb}$
		LOW/2.00E+17	0.00	$75,502/^n$
55	$CH_3OH(+M) = CH_3 + OH(+M)$	1.90E+16	0.00	$91,793^g$
		LOW/2.00E+17	0.00	$68,358/^k$
56	$CH_2 + H = H_2 + CH$	6.03E+12	0.00	$-1,788^d$
57	$CH_2 + O_2 = CO + H_2O$	2.41E+11	0.00	0^e
58	$CH_2 + O_2 = CH_2O + O$	3.29E+21	-3.30	$2,868^o$
59	$CH_2 + O_2 = HCO + OH$	4.30E+10	0.00	-500^i
60	$CH_2 + O_2 = CO + OH + H$	8.60E+10	0.00	-500^i
61	$CH_2 + O_2 = CO_2 + H_2$	2.63E+21	-3.30	$2,868^o$
62	$CH_2 + O_2 = CO_2 + H + H$	3.29E+22	-3.30	$2,868^o$
63	$CH_2 + O = CO + H_2$	6.00E+13	0.00	0^p
64	$CH_2 + O = CH + OH$	3.00E+14	0.00	$11,923^p$
65	$CH_2 + O = HCO + H$	3.02E+13	0.00	0^s
66	$CH_2 + O = CO + H + H$	7.26E+13	0.00	0^d
67	$CH_2 + OH = CH_2O + H$	1.81E+13	0.00	0^e
68	$CH_2 + OH = CH + H_2O$	4.50E+13	0.00	$3,000^i$
69	$CH_2 + H_2O_2 = CH_3 + HO_2$	6.03E+09	0.00	0^e
70	$CH_2 + H_2O = CH_3 + OH$	9.64E+07	0.00	0^e
71	$CH_2 + CH_2 = CH_3 + CH$	2.40E+14	0.00	$9,936^p$
72	$CH_2 + CH_2O = CH_3 + HCO$	6.03E+09	0.00	0^e
73	$CH_2 + CH_2OH = CH_3 + CH_2O$	1.21E+12	0.00	0^g
74	$CH_2 + HCO = CH_3 + CO$	1.81E+13	0.00	0^e
75	$CH_2 + CO_2 = CH_2O + CO$	2.35E+10	0.00	0^e
76	$CH_2 + CH_3O_2 = CH_2O + CH_3O$	1.81E+13	0.00	0^e
77	$CH_2(+M) = CH + H(+M)$	3.16E+15	0.00	$101,560^{bb}$
		LOW/4.00E+15	0.00	$83,065^q$
78	$CH_2O(+M) = H + HCO(+M)$	3.59E+14	0.00	$89,680^l$
		LOW/1.26E+16	0.00	$77,898/^d$
79	$CH_2O + H = H_2 + HCO$	2.29E+10	1.05	$3,279^d$
80	$CH_2O + O_2 = HCO + HO_2$	6.03E+13	0.00	$40,658^d$
81	$CH_2O + O = HCO + OH$	4.16E+11	0.57	$2,762^d$
82	$CH_2O + O = H + CO + OH$	6.03E+13	0.00	0^r
83	$CH_2O + OH = HCO + H_2O$	3.43E+09	1.18	-447^d
84	$CH_2O + HO_2 = CH_2OH + O_2$	3.39E+12	0.00	$19,121^s$
85	$CH_2O + HO_2 = H_2O_2 + HCO$	3.01E+12	0.00	$13,076^d$
86	$CH_2O + CH_3O_2 = CH_3O_2H + HCO$	1.99E+12	0.00	$11,665^e$
87	$CH_2O(+M) = H_2 + CO(+M)$	3.16E+13	0.00	$1,280^{bb}$
		LOW/4.52E+15	0.00	$35,300/^l$

P_{atm} denotes the standard-state pressure of one atmosphere; Z is the compressibility factor; T is the absolute temperature; R is the gas constant; ν_i is the stoichiometric coefficient of species i in the elementary reaction; and K_ϕ is the dimensionless equilibrium ratio given by

$$K_\phi = \Pi(\phi_i)^{\nu_i} \qquad (4)$$

where ϕ_i is the fugacity coefficient of species i.

CHEMKIN II treats the reacting mixture as an ideal gas, so Eq. 3 simplifies to

$$K_c = K_p \left(\frac{P_{atm}}{RT} \right)^{\Sigma \nu_i} \qquad (5)$$

when Z and ϕ_i are set equal to unity. Equation 5 was used in all simulations to obtain K_c. We also note here that CHEMKIN II, using the ideal gas law, required us to specify a pressure in the model that was higher than the experimental pressure so that CHEMKIN II would calculate the correct experimental density and species concentrations.

This ideal gas approximation in Eq. 5 is reasonably accurate for SCWO at high temperatures (around 600°C), but it

Table 1(continued). SCWO Mechanism with Kinetic Parameters

	Reactions[a]	A[b]	n	E_a^c
88	$CH_2OH + H = CH_3 + OH$	9.64E+13	0.00	0[g]
89	$CH_2OH + H = CH_2O + H_2$	6.03E+12	0.00	0[g]
90	$CH_2OH + O = CH_2O + OH$	4.22E+13	0.00	0[g]
91	$CH_2OH + HO_2 = H_2O_2 + CH_2O$	1.21E+13	0.00	0[g]
92	$CH_2OH + CH_2OH = CH_3OH + CH_2O$	4.82E+12	0.00	0[g]
93	$CH_2OH + HCO = CH_3OH + CO$	1.21E+14	0.00	0[g]
94	$CH_2OH + HCO = CH_2O + CH_2O$	1.81E+14	0.00	0[g]
95	$CH_2OH(+M) = CH_2O + H(+M)$	7.00E+14	0.00	29,637[i]
		LOW/4.51E+25	−2.50	34,190/[g]
96	$CH + H_2 = CH_3$	3.61E+10	0.00	−1,463[u,jj]
97	$CH + OH = HCO + H$	3.00E+13	0.00	0[i]
98	$CH + O = CO + H$	3.97E+13	0.00	0[d]
99	$CH + O_2 = HCO + O$	3.30E+13	0.00	0[i]
100	$CH + O_2 = CO + OH$	5.00E+13	0.00	0[v]
101	$CH + CO_2 = HCO + CO$	3.40E+12	0.00	690[i]
102	$CH + H_2O = CH_2OH$	5.71E+12	0.00	−755[w]
103	$HCO + H = H_2 + CO$	9.04E+13	0.00	0[d]
104	$HCO + O_2 = CO + HO_2$	5.12E+13	0.00	1,689[e]
105	$HCO + O = CO + OH$	3.01E+13	0.00	0[d]
106	$HCO + O = CO_2 + H$	3.01E+13	0.00	0[d]
107	$HCO + OH = H_2O + CO$	1.02E+14	0.00	0[d]
108	$HCO + HCO = CH_2O + CO$	3.01E+13	0.00	0[d]
109	$HCO(+M) = CO + H(+M)$	3.16E+15	0.00	15,270[bb]
		LOW/5.11E+21	−2.14	20,424/[e]
110	$CO + O_2 = CO_2 + O$	2.53E+12	0.00	47,693[e]
111	$CO + O(+M) = CO_2(+M)$	2.21E+14	0.00	10,470[l]
		LOW/6.17E+14	0.00	3,001/[e]
112	$CO + OH \Rightarrow H + CO_2$	1.17E+7	1.354	−725[dd]
		HIGH/2.45E−3	3.864	−1,234/[dd,kk]
		SRI/1.391	2,365	2,020/[dd]
113	$HOCO(+M) = H + CO_2(+M)$	1.74E+12	0.307	32,928[dd]
		LOW/2.29E+26	−3.024	35,074/[dd]
		SRI/2.490	5,755	1,601/[dd]
		K_c 1.23E−1	−0.01	8,700/[dd,ii]
114	$HOCO(+M) = OH + CO(+M)$	5.89E+12	0.53	33,981[dd]
		LOW/2.19E+23	−1.89	35,273/[dd]
		SRI/1.37	4,110	2,676/[dd]
		K_c 7.41E+5	−1.32	34,617/[dd,ii]
115	$HOCO + O_2 = CO_2 + HO_2$	1.00E+12	0.00	0[x]
116	$HOCO + HO_2 = CO_2 + H_2O_2$	1.00E+12	0.00	0[x]
117	$HOCO + CH_3O_2 = CO_2 + CH_3O_2H$	1.00E+12	0.00	0[x]
118	$CO + HO_2 = OH + CO_2$	1.51E+14	0.00	23,648[e]
119	$CO + CH_3O_2 = CH_3O + CO_2$	4.22E+06	0.00	0[y]
120	$CH_3O_2 + H_2 = CH_3O_2H + H$	3.01E+13	0.00	26,032[e]
121	$CH_3O_2 + H = CH_3O + OH$	9.64E+13	0.00	0[e]
122	$CH_3O_2 + O = CH_3O + O_2$	3.61E+13	0.00	0[e]
123	$CH_3O_2 + OH = CH_3OH + O_2$	6.03E+13	0.00	0[e]
124	$CH_3O_2 + HO_2 = CH_3O_2H + O_2$	4.63E+10	0.00	−2,583[e]
125	$CH_3O_2 + H_2O_2 = CH_3O_2H + HO_2$	2.41E+12	0.00	9,936[e]
126	$CH_3O_2 + CH_3O_2 = CH_3O + CH_3O + O_2$	6.88E+10	0.00	−219[z]

becomes less reliable as one approaches the critical temperature. To illustrate, as the temperature decreases from 700 to 400°C at 240 bar, Z decreases from 0.93 to 0.52. The solute fugacity coefficients for a 0.001 mole fraction solution of CO in H_2O and CH_4 in H_2O increase from 1.5 to 4.3 and from 1.3 to 2.2, respectively (Webley, 1989). Thus it is apparent that at the lower temperatures the ideal gas approximations made by CHEMKIN II will cause the model to become increasingly inaccurate. We note, however, that the compressibility factor differing from unity will affect only those reactions for which $\Sigma \nu_i \neq 0$. Fortunately, only three of the 17 most important reactions in Table 5 (discussed later) have $\Sigma \nu_i \neq 0$.

The fugacity coefficients differing from unity will affect the values of K_c for all reactions, but this effect may be comparable to the uncertainty in the estimate of k_f (Baulch et al., 1992; Tsang and Hampson, 1986). Moreover, all of the elementary reactions involve free radicals, and the fugacity coefficient for a free radical can be estimated only with great uncertainty (Schmitt et al., 1994). Thus, the uncertainty caused by the departure from ideal gas behavior may be unavoidable at the present time.

Three of the species in the model (CH_3O_2, CH_3O_2H, and HOCO) did not have thermodynamic information included in the CHEMKIN II database. We estimated the thermody-

Table 1(continued). SCWO Mechanism with Kinetic Parameters

	Reactions[a]	A^b	n	E_a^c
127	$CH_3O_2H + H = CH_3O + H_2O$	7.27E+10	0.00	3,720[aa]
128	$CH_3O_2H + OH = CH_3O_2 + H_2O$	7.23E+11	0.00	−258[d]
129	$H + H(+M) = H_2(+M)$	1.40E+12	0.50	0[j]
		LOW/9.78E+16	−0.60	0/[d]
130	$H + O_2(+M) = HO_2(+M)$	1.63E+13	0.00	761[cc]
		LOW/1.56E+18	−0.80	0/[d]
131	$H + O_2 = OH + O$	1.99E+14	0.00	16,812[d]
132	$H + OH = O + H_2$	4.88E+03	2.80	3,875[e]
133	$H + OH(+M) = H_2O(+M)$	1.62E+14	0.00	149[cc]
		LOW/1.41E+23	−2.00	0/[d]
134	$H + HO_2 = OH + OH$	1.69E+14	0.00	874[d]
135	$H + HO_2 = H_2 + O_2$	4.28E+13	0.00	1,411[d]
136	$H + HO_2 = O + H_2O$	3.01E+13	0.00	1,721[d]
137	$H + H_2O_2 = H_2 + HO_2$	1.69E+12	0.00	3,756[d]
138	$H + H_2O_2 = OH + H_2O$	1.02E+13	0.00	3,577[d]
139	$H + H_2O = H_2 + OH$	4.52E+08	1.60	18,421[d]
140	$O + H(+M) = OH(+M)$	1.03E+13	0.50	0[j]
		LOW/4.71E+18	−1.00	0/[e]
141	$O + O(+M) = O_2(+M)$	7.64E+12	0.50	0[j]
		LOW/1.89E+13	0.00	−1,788/[e]
142	$O + HO_2 = OH + O_2$	3.25E+13	0.00	0[d]
143	$O + H_2O_2 = OH + HO_2$	9.63E+06	2.00	3,974[e]
144	$O + H_2O = OH + OH$	4.58E+09	1.30	17,100[e]
145	$HO_2 + HO_2 = O_2 + H_2O_2$	4.20E+14	0.00	6,030[ee]
	second exponential	1.30E+11	0.00	820[ee]
146	$H_2O_2(+M) = OH + OH(+M)$	3.00E+14	0.00	48,488[d]
		LOW/1.21E+17	0.00	45,507/[d]
		TROE/$F_c = 0.5/$[d]		
147	$OH + HO_2 = H_2O + O_2$	2.89E+13	0.00	−497[d]
148	$OH + H_2O_2 = HO_2 + H_2O$	7.83E+12	0.00	1,331[d]

[a]Species[ff]: CH_4 $CH_3O_2H^{gg}$ $CH_3O_2^{gg}$ CH_3OH CH_3O CH_3 CH_2OH CH_2O CH_2 $HOCO^{gg}$ HCO CH CO CO_2 O_2 O H_2 H H_2O OH HO_2 H_2O_2
[b]Units of mol, cc, and seconds.
[c]cal/mol, $k = AT^n \exp(-E_a/RT)$.
[d]Baulch et al. (1992).
[e]Tsang and Hampson (1986).
[f]Bohland et al. (1985).
[g]Tsang (1987).
[h]Dean and Westmoreland (1987).
[i]Glarborg et al. (1986).
[j]Hard spheres collision rate.
[k]Warnatz, 1984.
[l]Mean of all values in Mallard et al. (1993).
[m]Mean of all values in Mallard et al. (1993) except Basevich et al. (1975).
[n]Hidaka et al. (1989).
[o]Dombrowsky and Wagner (1992).
[p]Frank and Just (1984).
[q]Dean and Hanson (1992).
[r]Dean and Kistiakowsky (1970).
[s]Tsuboi and Hashimoto (1981).

[t]Greenhill et al. (1986).
[u]Becker et al. (1991).
[v]Lichtin et al. (1983).
[w]Zabarnick et al. (1988).
[x]Reaction rate based on analogy with $HOCH_2 + O_2 = CH_2O + HO_2$.
[y]Sander and Watson (1980).
[z]Wallington et al. (1992).
[aa]Slemr and Warneck (1977).
[bb]Estimated using recommendation of Senkan (1992).
[cc]Cobos and Troe (1985).
[dd]Larson et al. (1988a,b).
[ee]Rate constant calculated as sum of two temperature-dependent exponentials as recommended by Hippler et al. (1990).
[ff]Thermodynamics from Kee et al. (1991) unless otherwise noted.
[gg]Thermodynamics based on estimate using Benson (1976) and THERM.
[hh]Stewart et al. (1989).
[ii]SRI equilibrium constant used to calculate reverse rate $K_c(mol/cm^3) = \alpha T^\beta \exp(-\gamma/RT)$ where γ is in cal/mol.
[jj]Only high-pressure data.
[kk]High-pressure limit is pressure-dependent (Larson et al., 1988a).

namic properties for these species using Benson's (1976) group additivity method as implemented in THERM (Ritter and Bozzelli, 1991).

Pressure effects

The rates of unimolecular, gas-phase reactions are pressure (density) dependent. The reactant, A, requires a collision partner, typically denoted as M, to transfer enough energy for a reaction to occur. Such a system can be represented as two elementary reactions that involve an energized intermediate, A^*, as shown below.

$$A + M \underset{-1}{\overset{1}{\rightleftharpoons}} A^* + M \qquad (6)$$

$$A^* \overset{2}{\rightarrow} \text{products.} \qquad (7)$$
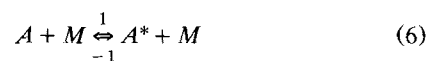
The rate of disappearance of reactant A is

$$-r_A = k_1[A][M] - k_{-1}[A^*][M] \qquad (8)$$

where k_1 and k_{-1} are the rate constants for the forward and reverse reaction in Eq. 6, respectively. Invoking the quasi-sta-

Table 2. Reactions in Table 1 with Pressure-Dependent Kinetics[a]

Reaction	$k_0[M]$ (1/s)	k_∞ (1/s)	k_{uni} (1/s)
$CH_4(+M) = CH_3 + H(+M)$	8.12E − 11	2.01E − 14	2.01E − 14
$CH_3 + O_2(+M) = CH_3O_2(+M)$	8.36E + 13	2.29E + 12	1.53E + 12
$CH_3(+M) = CH_2 + H(+M)$	1.20E − 12	3.01E − 16[b]	3.01E − 16
$CH_3O(+M) = CH_2O + H(+M)$	3.30E + 7	1.28E + 7	9.24E + 6
$CH_3OH(+M) = CH_2OH + H(+M)$	4.41E − 7	2.27E − 12[b]	2.27E − 12
$CH_3OH(+M) = CH_3 + OH(+M)$	4.61E − 5	2.12E − 10	2.12E − 10
$CH_2(+M) = CH + H(+M)$	6.41E − 11	6.11E − 14[b]	2.12E − 10
$CH_2O(+M) = HCO + H(+M)$	5.82E − 9	1.59E − 11	1.58E − 11
$CH_2O(+M) = H_2 + CO(+M)$	2.31E + 3	1.37E + 13[b]	2.31E + 3
$CH_2OH(+M) = CH_2O + H(+M)$	2.86E + 6	2.92E + 6	1.45E + 6
$HCO(+M) = CO + H(+M)$	2.77E + 7	1.52E + 11[b]	2.77E + 7
$CO + O(+M) = CO_2(+M)$	4.28E + 11	2.42E + 11	1.55E + 11
$CO + OH(+M) \Rightarrow H + CO_2(+M)$	1.53E + 11	9.99E + 12	2.93E + 10
$HOCO(+M) = H + CO_2$	1.23E + 3	6.56E + 3	5.58E + 3
$HOCO(+M) = OH + CO_2$	1.94E + 3	4.94E + 4	3.76E + 4
$H + H(+M) = H_2(+M)$	8.85E + 12	3.89E + 13[b]	7.21E + 12
$H + O_2(+M) = H_2O(+M)$	3.73E + 13	9.93E + 12	7.84E + 12
$H + OH(+M) = HO_2(+M)$	1.15E + 15	1.47E + 14	1.30E + 14
$O + H(+M) = OH(+M)$	2.98E + 13	2.86E + 14[b]	2.70E + 13
$O + O(+M) = O_2(+M)$	2.96E + 11	2.12E + 14[b]	2.96E + 11
$H_2O_2(+M) = 2OH(+M)$	1.47E + 2	5.87E + 0	4.30E + 0

[a]The rate constants are the low-pressure limit $(k_0[M])$; the high-pressure limit (k_∞); and k_{uni} from Eq. 11 or 12 at 500°C and $[H_2O] = 4.89E − 3$ mol/cm^3.
[b]Estimated k_∞, see text.

tionary-state approximation for A^* and making the appropriate substitutions, one can rewrite Eq. 8 as

$$- r_A = \frac{k_1 k_2[M]}{k_{-1}[M] + k_2}[A] = k_{uni}[A]. \qquad (9)$$

At low pressures, collisions are infrequent and the rate of energy transfer limits the net reaction rate $(k_{-1}[M] \ll k_2)$. The pseudo-first-order rate constant (k_{uni}) in this low-pressure limit is often termed $k_0[M]$, where $k_0 = k_1$ in Eq. 9. The rate constant at the low-pressure limit, $k_0[M]$, varies linearly with pressure since the collision partner is important under these conditions. At high pressures, collisions are more frequent, and energy transfer is more rapid $(k_{-1}[M] \gg k_2)$, so k_{uni} approaches a limiting value of k_∞ (which is not a function of $[M]$) at a given temperature. Using the notation in Eq. 9, $k_\infty = k_1 k_2/k_{-1}$.

Different reactants reach their high-pressure limit at different pressures depending on the reactant's ability to store and transfer internal energy. Complex molecules of 10 atoms or more reach their high-pressure limits at relatively low pressures since they can distribute energy in vibrational or rotational excited states (Senkan, 1992). The energy in these excited states can be used to overcome the energy of activation. For recombination reactions (the reverse of the unimolecular dissociation) the energy liberated by the reaction can be distributed within these intramolecular degrees of freedom, thereby preventing the transition state species from dissociating before a reaction occurs. Small molecules or atoms do not have many vibrational or rotational degrees of freedom, so their high-pressure limit occurs at pressures much higher than those for complex molecules. In fact many atom–atom recombination reactions have not had their high-pressure kinetics determined experimentally because of the extreme pressures involved.

We used the Lindemann model to account for this pressure dependence for unimolecular reactions in this model. The reactions so affected are listed in Table 2. Previous models for SCWO (Holgate and Tester, 1994b) included the pressure dependence of only a few reactions. Other unimolecular reactions were taken to be in either their high- or low-pressure limits.

The apparent unimolecular rate constant over the entire pressure range, k_{uni}, is determined from the Lindemann model as

$$\frac{1}{k_{uni}} = \frac{1}{k_0[M]} + \frac{1}{k_\infty}. \qquad (10)$$

This form is convenient for determining k_{uni} from tabulated k_0 and k_∞. Rearranging, the rate constant is given as

$$k_{uni} = \frac{k_0 k_\infty[M]}{k_0[M] + k_\infty}. \qquad (11)$$

A graphical representation of the effect of pressure (density) on k_{uni} is shown in Figure 1. The Lindemann model in Eq. 11 is very simple, but it is not accurate quantitatively. To model pressure effects more accurately, yet retain the convenience of the analytical Lindemann formulation, we modified the Lindemann model with a broadening parameter, F:

$$k_{uni} = \frac{k_0 k_\infty[M]}{k_0[M] + k_\infty} F. \qquad (12)$$

The broadening parameter can be determined from RRKM calculations (Steinfeld, 1989). Troe (1977), Gilbert et al. (1983), and a group at SRI (Stewart et al., 1989) provide cor-
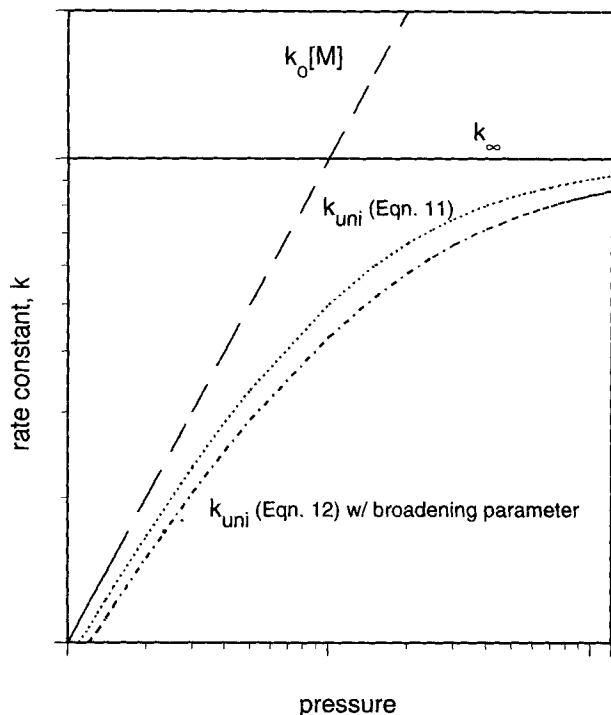
Figure 1. Log-log plot of apparent first-order rate constants based on the Lindemann model.

relations for the broadening parameter that can be used in detailed chemical kinetics models. Including the broadening parameter causes the k_{uni} curve to fall below that of the simple Lindemann formulation, as illustrated in Figure 1.

We included values of k_∞ for all unimolecular reactions in the model. We estimated these values when experimental data were unavailable. Including values of k_∞ is important because doing so prevents the model from extrapolating the low-pressure limit kinetics to high pressures and obtaining unrealistically high reaction rates, as seen in Figure 1. We estimated the high-pressure limit reaction rate coefficient for atom–atom recombination reactions using Eq. 13, which arises from hard-spheres collision theory:

$$k_\infty = \frac{Z_{AB}}{\rho_A \, \rho_B} = (\pi r_{AB}^2) \left[\frac{8 k_B T}{\pi \left(\dfrac{m_A m_B}{m_A + m_B} \right)} \right]^{1/2} \tag{13}$$

where Z_{AB} is the collision frequency; ρ_A and ρ_B are the number density of A and B; r_{AB} is the sum of the radii of the two reactants; m_A and m_B are the masses of the reacting molecules; and k_B is Boltzmann's constant.

We used the recommendations of Senkan (1992) to estimate k_∞ for simple and complex fission reactions that did not have their high-pressure limit rate constants reported in the literature. Simple fission reactions form two radicals by breaking a single bond in an energized molecule. For simple fission reactions we took the preexponential factor to be $10^{15.5}$ s^{-1} and the activation energy to be equal to the heat of reaction, ΔH_r. Complex radical and molecular fissions involve the

concerted breakage and formation of multiple bonds. The preexponential factors for the radical and molecular fissions were approximated as $10^{13.2}$ and 10^{13} s^{-1}, respectively. The activation energies were approximated as ΔH_r and $\Delta H_r + 5$ kcal/mol, respectively. We note that more accurate estimates, if desired, could be obtained from the application of transition state theory (Benson, 1976).

Reactions for which we used estimated values of k_∞ are so noted in Table 2. This table also compares the apparent unimolecular reaction rate constant calculated from Eq. 11 (or Eq. 12 if applicable) with the low-pressure rate constant extrapolated to SCWO conditions. It is apparent that simply extrapolating the low-pressure limit gives rate constants that are too high for several of the reactions.

The rates of some nominally bimolecular reactions can also exhibit a pressure dependence. For example, the reaction

$$CO + OH = CO_2 + H \tag{14}$$
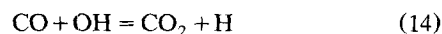
proceeds through a chemically activated intermediate, HOCO. The activated intermediate can proceed on to form $CO_2 + H$, or it can be deactivated and stabilized through intermolecular collisions. Thus, the HOCO formation and destruction rates are pressure dependent. We used the RRKM results of Larson et al. (1988a) for this reaction. These authors suggest that reaction 14 be written as three elementary reactions.

$$CO + OH \Rightarrow CO_2 + H \tag{15}$$

$$CO + OH = HOCO \tag{16}$$

$$CO_2 + H = HOCO \tag{17}$$
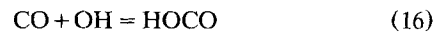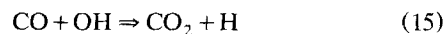
All three reactions have pressure-dependent rates that were modeled with high- and low-pressure limits and with SRI broadening parameters. The rate constants for the reverse of reactions 16 and 17 are calculated with parameters for equilibrium constants provided by Larson et al. (1988a,b). These parameters are listed in Table 1.

In addition to reaction 17, our model includes other pathways for the conversion of HOCO to CO_2. These steps involve attack by different peroxy radicals such as O_2, HO_2, and CH_3O_2. The rates of these reactions are not available in the literature. The reaction rate constant for each of these steps was approximated as 10^{12} cm^3/mol·s based on their similarity to the reaction

$$CH_2OH + O_2 = CH_2O + HO_2 \tag{18}$$
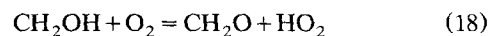
and its associated kinetics (Mallard et al., 1993). The precise values of these rate constants had an insignificant effect on the model results. More refined estimates of the rate constants, if desired, could be obtained through QRRK calculations (Dean and Westmoreland, 1987).

Model Results

We used the model described in the previous section to predict the results of SCWO experiments reported in the literature. This section describes the ability of the model to
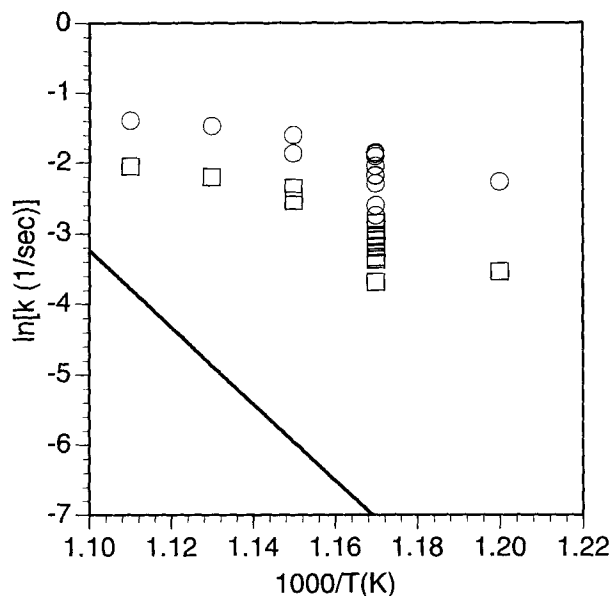
Figure 2. Arrhenius plot for SCWO of methane.

The squares are experimental data (Webley and Tester, 1991); the circles are the predictions of the present model; and the line is the prediction of the model of Webley and Tester (1991).

predict the SCWO kinetics for methane, methanol, CO, and H_2.

Methane oxidation

Webley and Tester (1991) published experimental kinetics data for the SCWO of methane. They give the methane conversion, X, obtained at several specific sets of reaction conditions. We used these specific reaction conditions in our model and predicted the methane conversion. We then calculated a pseudo-first-order rate constant, k, as

$$k = \frac{-\ln(1 - X)}{\tau} \qquad (19)$$

where τ is the reactor residence time. Figure 2 summarizes the results of the experiments (squares), the predictions of our model (circles), and the predictions of the model of Webley and Tester (1991) (solid line) on an Arrhenius plot. Our model predicts rate constants that are higher than the experimental values, but the two sets of data have similar slopes, indicating that they have similar energies of activation. Furthermore, the present model provides a better prediction of the experimental results than does the model of Webley and Tester.

There is some scatter in the rate constants obtained at the same temperature in Figure 2. This scatter appears because using pseudo-first-order kinetics for methane does not correctly account for the effect of the O_2 concentration on the reaction rate. Webley and Tester (1991) found that the kinetics are 0.99 order in methane and 0.66 order in oxygen. We used these reported reaction orders as another test of our mechanistic model. We made several model runs to explore the effect of the CH_4 concentration on the initial oxidation
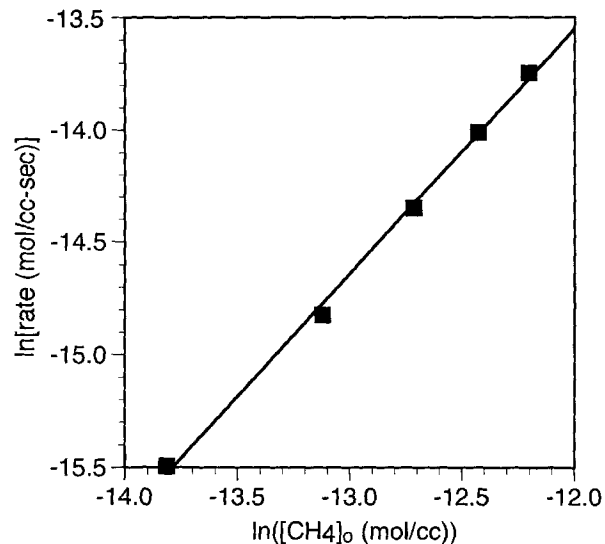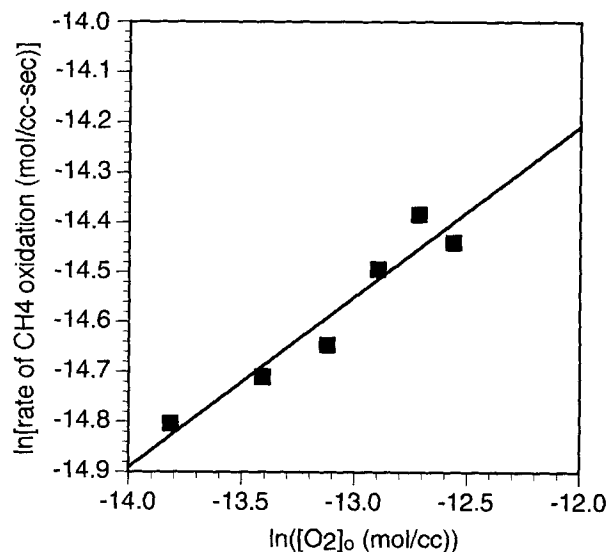

Figure 3. Initial rate of CH_4 oxidation as a function of the initial CH_4 concentration.

Model conditions: $[O_2]_0 = 4.00E - 6$ mol/cm^3, $[H_2O]_0 = 3.85E - 3$ mol/cm^3, $T = 873$ K.

rate of CH_4. All of these model runs were done at the same temperature (873 K) and O_2 concentration ($4.0E - 6$ mol/cm^3), using conditions that were representative of those used experimentally. The initial rate of methane oxidation, $rate_0$, was calculated by

$$rate_0 = \frac{[CH_4]_0 X}{\tau}. \qquad (20)$$

Conversions were kept below 10% so that the initial rate would be measured. This initial rate was then plotted against the initial concentration of CH_4 on log-log coordinates, as shown in Figure 3. The slope of the best-fit line through these

Figure 4. Initial rate of CH_4 oxidation as a function of the initial O_2 concentration.

Model conditions: $[CH_4]_0 = 3.00E - 6$ mol/cm^3, $[H_2O]_0 = 3.85E - 3$ mol/cm^3, $T = 873$ K.

Table 3. Comparison of the Experimental Reaction Orders[a] with the Reaction Orders Predicted by the Model for the Fuel and O_2

	Experimental		Model	
Compound	Fuel	O_2	Fuel	O_2
Methane[b]	0.99 ± 0.08	0.66 ± 0.14	1.09 ± 0.10^f	0.34 ± 0.14^j
Methanol[c]	0.89 ± 0.69	0.12 ± 0.66	1.23 ± 0.11^g	0.00 ± 0.05^j
CO[d]	0.96 ± 0.30	0.34 ± 0.24	0.86 ± 0.04^h	0.02 ± 0.05^k
H_2[e]	1.10 ± 0.25	0.02 ± 0.29	0.86 ± 0.13^i	0.00 ± 0.10^k

[a] Webley and Tester, 1991; Tester et al., 1993; Holgate and Tester, 1993, 1994a.
[b] $T = 873$ K, $[H_2O] = 3.85E - 3$ mol/cm³.
[c] $T = 766$ K, $[H_2O] = 5.00E - 3$ mol/cm³.
[d] $T = 770$ K, $[H_2O] = 4.93E - 3$ mol/cm³.
[e] $T = 823$ K, $[H_2O] = 4.28E - 3$ mol/cm³.
[f] $[O_2]_0 = 4.00E - 6$ mol/cm³.
[g] $[O_2]_0 = 3.00E - 6$ mol/cm³.
[h] $[O_2]_0 = 1.50E - 6$ mol/cm³.
[i] $[O_2]_0 = 1.00E - 6$ mol/cm³.
[j] $[fuel]_0 = 3.00E - 6$ mol/cm³.
[k] $[fuel]_0 = 1.50E - 6$ mol/cm³.

data indicates that the methane order is 1.09 ± 0.10 for the model. The uncertainty gives the 95% confidence interval. The results of a similar analysis to determine the O_2 reaction order are shown by Figure 4. Linear regression of these data leads to an O_2 order of 0.34 ± 0.14. Both of these values appear in Table 3, where they are compared to the experimental values. The predicted order for CH_4 agrees with the experimental value. The predicted order for oxygen, however, is about half of the experimental value.

Webley and Tester (1991) also published CO_2 selectivities for their different methane oxidation experiments. Our model overpredicted the CO_2/CO ratio in all cases, just as it had overpredicted the rate of methane oxidation. The oxidation of CO and some remedies for this overprediction are discussed later.

Methanol oxidation

Data from Tester et al. (1993) were used to test the model's predictions for methanol oxidation in SCW. Figure 5 is an Arrhenius plot with pseudo-first-order rate constants for methanol. The circles are the predictions of our model, the squares are the experimental data, and the solid line is the prediction of a model by Webley et al. (1990). Our model predicts rate constants that are too high, and it predicts an activation energy that is too low. One reason that the model does not perform as well for methanol as it did for methane may be that the methanol experiments were run at lower temperatures than were the methane experiments. Indeed the highest temperature used in the methanol experiments is lower than the lowest temperature used in the methane experiments. We noted previously that the closer one is to the critical point the worse the ideal gas approximations used in the model become.

We also used the model to predict the global reaction orders for methanol and O_2 for methanol oxidation. The model correctly predicted that the reaction order for O_2 is zero. Table 3 also shows that the experimental and predicted reaction orders for methanol are within experimental uncertainty of each other.
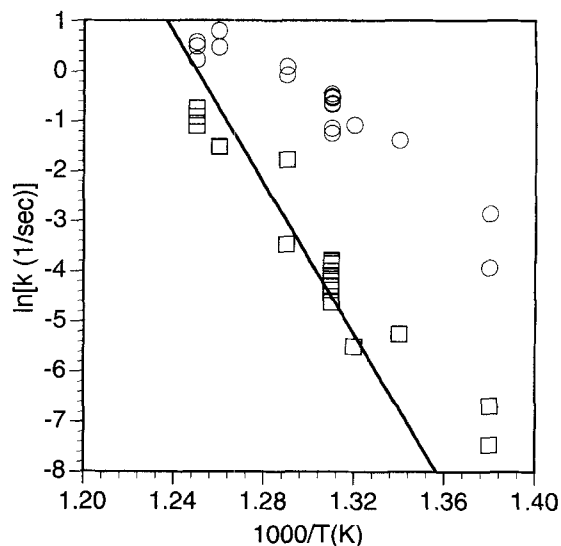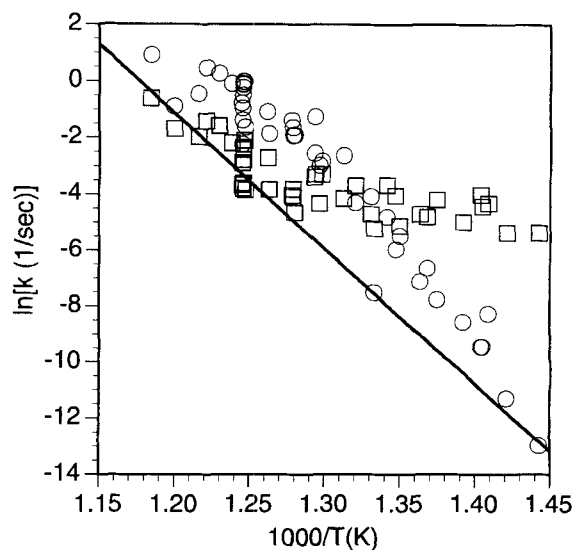

Figure 5. Arrhenius plot for SCWO of methanol.

The squares are experimental data (Tester et al., 1993); the circles are the predictions of the present model; and the line is the prediction of the model of Webley et al. (1990).

CO oxidation

Experimental results for CO oxidation were taken from Holgate et al. (1992) and Holgate and Tester (1994a). Figure 6 provides an Arrhenius plot of pseudo-first-order rate constants for CO. Again, circles represent the predictions of the present model, squares are experimental data, and the solid line is the prediction of a model by Holgate and Tester (1994b). At the higher temperatures, which are similar to those used in the methane experiments, the predicted CO oxidation rate is too fast, but the activation energy is very similar for both the experimental results and the model. As

Figure 6. Arrhenius plot for SCWO of CO.

The squares are experimental data (Holgate et al., 1992); the circles are the predictions of the present model; and the line is the prediction of the model of Holgate and Tester (1994b).

Figure 7. Arrhenius plot for SCWO of H_2.

The squares are experimental data (Holgate and Tester, 1993); the circles are the predictions of the present model; and the line is the prediction of the model of Holgate and Tester (1993).
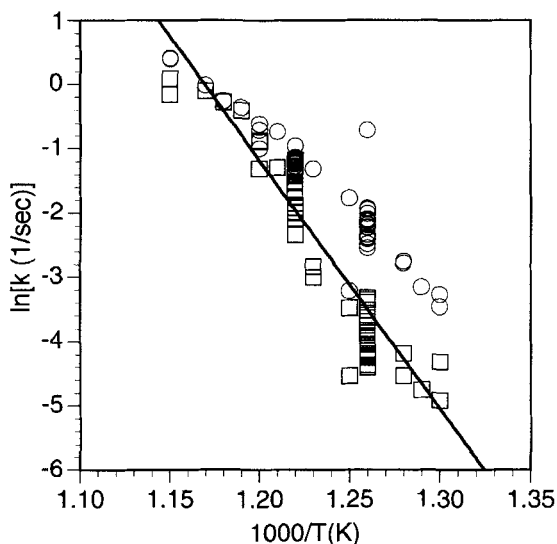

Figure 8. Effect of residence time on H_2 conversion by SCWO at 550°C and $[H_2O] = 4.25E\text{-}3$ mol/cm^3.

The points show the experimental data (Holgate and Tester, 1993), while the lines show model predictions. The squares and the solid line correspond to $[H_2]_0 = 1.07E - 6$ mol/cm^3. $[O_2]_0 = 0.54E - 6$ mol/cm^3; the circles and dashed line correspond to $[H_2]_0 = 2.06E - 6$ mol/cm^3, $[O_2]_0 = 1.04E - 6$ mol/cm^3; and the triangles and the dotted line correspond to $[H_2]_0 = 3.06E - 6$ mol/cm^3, $[O_2]_0 = 1.55E - 6$ mol/cm^3.
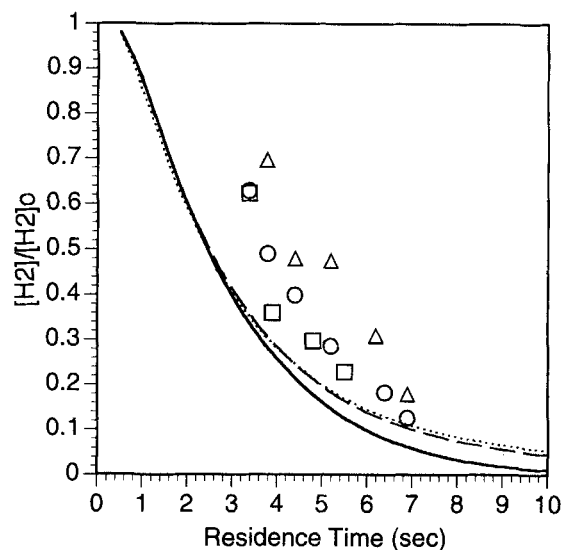
the temperature decreases, however, the activation energy for the experimental data appears to decrease. This causes the model to underpredict CO oxidation at lower temperatures. CO oxidation was unique in this respect when compared to the other compounds studied. Table 3 shows that the model predicted the CO reaction order to within experimental uncertainty. The model predicted no effect of O_2 on the rate, but a small effect was observed experimentally.

Holgate and Tester (1994b) also developed a model for CO oxidation. Their model gave good predictions of experimental results for fuel-rich and stoichiometric feeds at 550 K, but it did a poorer job for fuel-lean mixtures and for lower temperatures. Of course, fuel-lean mixtures would be the type encountered in a commercial SCWO unit. One of the key reasons that the predictions of our model differ from those of Holgate and Tester is that we used different values for the standard heat of formation of HO_2. We discuss this point more fully later.

H_2 oxidation

Figure 7 compares the model predictions (circles) with the experimental results (squares) (Holgate and Tester, 1993) for H_2 oxidation in SCW. At high temperatures the model does an excellent job of reproducing the experimental results, but as the temperature decreases toward the critical point the experimental results and model predictions begin to diverge. This divergence may be due to the model's use of the ideal gas law. Table 3 shows that the model predicted the H_2 and O_2 global reaction orders to within their experimental uncertainties.

One potential problem with using pseudo-first-order rate constants to compare the predicted and experimental kinetics results for the SCWO of H_2 is that H_2 oxidation exhibits an induction period (Holgate and Tester, 1993). That is, a pe-

riod of time exists during which very little hydrogen is consumed. After this induction period ends, however, the oxidation rate becomes rapid and the H_2 concentration decreases in a nearly exponential decay. It is instructive to compare model predictions and experimental results for this induction time and for the kinetic decay constant for H_2 disappearance.

Figure 8 displays several sets of data for different H_2 concentrations. All of these data were obtained using a stoichiometric H_2/O_2 feed. In all cases the model predicted H_2 concentrations that were much lower than the experimental concentrations (Holgate and Tester, 1993). The shapes of the curves are very similar, however, indicating that the oxidation rate is being correctly modeled, but that the predicted induction time is too short. Figure 9 examines this aspect more closely. Data for the model and experiments have been plotted for an initial H_2 concentration of $3.06E - 6$ mol/cm^3 for ratios of $[H_2]/[H_2]_0$ between 0.7 and 0.1. Both sets of data were then fit with exponential curves. The curve through the experimental data is

$$\frac{[H_2]}{[H_2]_0} = 3.06\exp(-0.393\tau), \tag{21}$$

whereas the curve through the model predictions is

$$\frac{[H_2]}{[H_2]_0} = 1.20\exp(-0.361\tau) \tag{22}$$

where τ is in seconds. The constants multiplying the residence time in the exponential terms are within 8% of each
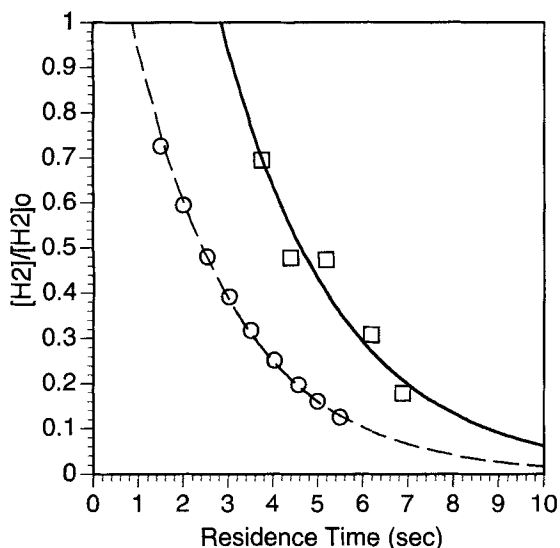
Figure 9. Effect of residence time on H_2 conversion by SCWO at 550°C, $[H_2O] = 4.25E\text{-}3$ mol/cm^3, $[H_2]_0 = 3.06E\text{-}6$ mol/cm^3, and $[O_2]_0 = 1.55E\text{-}6$ mol/cm^3.

The squares are experimental data (Holgate and Tester, 1993), and the circles are the predictions of the present model. Both sets of data are fit with exponential curves.

other. This shows good agreement for the model and experimental kinetic decay constants at these conditions. The induction time for the experimental run is 2.8 s, compared to the model's predicted induction time of 0.9 s.

To summarize, this section compared the model predictions with experimental kinetics data in the literature for the SCWO of methane, methanol, CO, and hydrogen. Pseudo-first-order rate constants from the model were generally higher than the experimental values. The model gave accurate (within the uncertainty) predictions of the global reaction orders for the four fuels and of the oxygen reaction orders for two of the fuels. The model accurately predicted that methane oxidation rate would be the most sensitive to the oxygen concentration. The model accurately predicted the activation energy for methane oxidation and for the oxidation of hydrogen and CO at high temperatures. The model predictions enjoyed the best agreement with experimental results at high temperatures.

Sensitivity Analysis

The quantitative predictions of the detailed chemical kinetics model depend on the numerical values of the parameters used. None of the reaction rate constants are known with absolute certainty, however, so it is important to examine the effect of small changes in the rate constants on the calculated species concentrations. Therefore, we have conducted a sensitivity analysis for the SCWO of CH_4, CH_3OH, CO, and H_2. We used SENKIN (Lutz et al., 1991), a FORTRAN program that is part of the CHEMKIN package to perform the sensitivity analysis. The results of the sensitivity analysis are given in terms of a matrix of normalized sensitivity coefficients, S_{ij}, defined as

$$S_{ij} = \frac{\partial \ln x_i}{\partial \ln k_j} \tag{23}$$

where x_i is the mole fraction of species i, and k_j is the forward rate constant for reaction j at a given set of reaction conditions (such as temperature, pressure, and concentration of species). A positive sensitivity coefficient indicates that the forward reaction helps form the species being evaluated, whereas a negative sensitivity coefficient indicates that the forward reaction helps consume the species under question.

Comparing the absolute values of the sensitivity coefficients for a given species allows one to identify the reactions that most strongly influence the concentration calculated for that compound. We used the results of our sensitivity analysis to identify the most important reactions for modeling the disappearance of methane, methanol, CO, and hydrogen during SCWO. Table 4 summarizes these results, and several important points emerge from the sensitivity analysis.

We first note that although the mechanism contains 148 reactions, only a much smaller subset of these reactions strongly influences the oxidation kinetics of the compounds studied (under these conditions). Another important point that the sensitivity analysis revealed is that some of the reactions appearing in Table 4 have not been included in previous detailed chemical kinetic models for SCWO. The reactions included in our model that others have omitted are

$$HOCO = CO + OH \tag{24}$$

$$CH_3 + O_2 = CH_2O + OH \tag{25}$$

$$CH_3OH + OH = H_2O + CH_3O \tag{26}$$
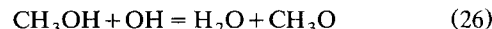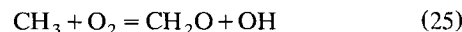
Most of the reactions in Table 4 are nominally bimolecular, and, the sum of the stoichiometric coefficients is zero. This observation indicates that the compressibility of water departing from unity and the precise way pressure-dependent reactions were modeled will have an important effect only on the three unimolecular reactions and any chemically activated reactions in Table 4.

We also note that nearly half of the reactions in Table 4 involve HO_2. We noted earlier that we used a value for ΔH_f (298 K) for HO_2 (2.0 kcal/mol) that was higher than the value of 0.499 kcal/mol used in other recent models (Holgate and Tester, 1993, 1994b). Our value was taken from the CHEMKIN thermodynamic database, whereas Tester's group used the value in the JANAF tables (Chase et al., 1985). The value in the CHEMKIN database is in better agreement with recent reported values of ΔH_f (298 K) for HO_2 (see Holgate and Tester, 1994b, and references therein), so we feel it is a more reliable value than the JANAF value. Moreover, the uncertainty ascribed to the JANAF value of 0.499 ± 2 kcal/mol is quite large. Holgate and Tester (1993, 1994b) noted that using values of ΔH_f (298 K) for HO_2 higher than the JANAF value caused the predicted oxidation rates for CO and H_2 to increase and become more rapid than the experimental rates. They obtained the good agreement in Figures 6 and 7 by using the lower JANAF value for ΔH_f (298 K) for HO_2. It is clear that the thermochemical data for HO_2 are important for correctly modeling SCWO kinetics.

Table 4. Normalized Sensitivity Coefficients for CH_4, CH_3OH, CO, and H_2 for the Most Important Elementary Reactions

	$CH_4{}^a$	CH_3OH^b	CO^c	$H_2{}^d$
$OH+HO_2 = H_2O+O_2$	2.56E−1	1.20E−2	4.66E−3	1.79E−1
$CH_3+HO_2 = CH_3O+OH$	−2.26E−1			
$OH+H_2O_2 = HO_2+H_2O$	−1.73E−1		−2.09E−1	−2.18E−1
$HO_2+HO_2 = O_2+H_2O_2$	8.15E−2	7.59E−2	1.05E−1	7.72E−2
$CH_4+OH = CH_3+H_2O$	−4.69E−2			
$CH_3+O_2 = CH_2O+OH$	−3.52E−2			
$H_2O_2+M = OH+OH+M$	−2.47E−2	−1.15E−1	−1.52E−1	−1.41E−1
$H+H_2O = H_2+OH$	1.03E−2	8.09E−3		−2.69E−1
$CH_4+HO_2 = H_2O_2+CH_3$	−6.09E−3			
$OH+CO+M \Rightarrow HOCO+M$	−1.79E−3	1.79E−2	−1.32E−2	
$CH_3OH+HO_2 = H_2O_2+CH_2OH$		−1.13E−1		
$CH_3OH+OH = H_2O+CH_2OH$		−5.55E−2		
$CH_3OH+OH = H_2O+CH_3O$		−3.24E−2		
$CH_2O+HO_2 = CH_2OH+O_2$		−9.63E−3		
$CO+HO_2 = OH+CO_2$			−5.18E−2	
$O+H_2O = OH+OH$			−1.01E−3	
$H+O_2+M = HO_2+M$				−3.77E−2

$^a CH_4$ conditions: $T = 873$ K, $[CH_4]_0 = 1.67E−6$ mol/cm^3, $[O_2]_0 = 3.24E−6$ mol/cm^3, $[H_2O] = 3.85E−3$ mol/cm^3, $\tau = 5$ s.
$^b CH_3OH$ conditions: $T = 776$ K, $[CH_3OH]_0 = 2.16E−6$ mol/cm^3, $[O_2]_0 = 2.04E−6$ mol/cm^3, $[H_2O] = 4.84E−3$ mol/cm^3, $\tau = 4.5$ s.
$^c CO$ conditions: $T = 781.5$ K, $[CO]_0 = 2.04E−6$ mol/cm^3, $[O_2]_0 = 2.04E−6$ mol/cm^3, $[H_2O] = 4.77E−3$ mol/cm^3, $\tau = 3.0$ s.
$^d H_2$ conditions: $T = 842$ K, $[H_2]_0 = 1.21E−6$ mol/cm^3, $[O_2]_0 = 9.85E−7$ mol/cm^3, $[H_2O] = 4.4E−3$ mol/cm^3, $\tau = 4.5$ s.

Methane oxidation revisited

The sensitivity analysis for SCWO of methane in Table 4 revealed that the three most important reactions for determining the oxidation rate were

$$CH_3 + HO_2 = CH_3O + OH \qquad (27)$$

$$OH + HO_2 = H_2O + O_2 \qquad (28)$$

$$OH + H_2O_2 = HO_2 + H_2O \qquad (29)$$
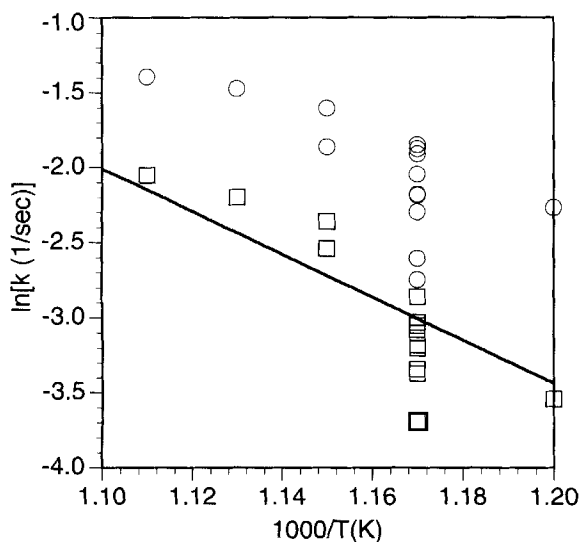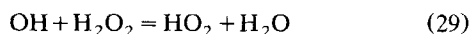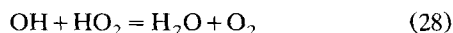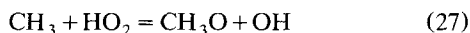
Figure 10. Arrhenius plot for SCWO of methane.

The squares are experimental data (Webley and Tester, 1991); the circles are the predictions of the original model; and the line is the prediction of the model after adjusting three preexponential factors as described in the text.

By adjusting the preexponential factors of these three reactions within their uncertainties, we were able to get good agreement between the experimental results and the model predictions, as shown by the solid line in Figure 10. The adjustments we made were to multiply the preexponential factors by 0.5, 2.0, and 0.9, respectively.

This exercise shows that the model, within its uncertainty, can predict the experimental SCWO kinetics for methane. The exercise also shows how a sensitivity analysis and experimental SCWO data can be used to get better estimates of the rate constants for elementary reactions. Of course, the predictions of the adjusted model must be compared with many additional experimental data to confirm the general utility of the adjustments. This work is in progress.

We return now to the issue of the standard heat of formation of the HO_2 radical. Since our model and previous models used different values for ΔH_f (298 K) for HO_2, the equilibrium constant and reverse rate constant for every reaction that contains HO_2 radicals must also differ. The effect of these differences can be important, as shown by Figure 11. Here we plot experimental (Webley and Tester, 1991) and predicted methane conversions for different versions of our model. Circles show the predictions of the original model with the parameters taken directly from the literature as they appear in Table 1. The squares show the model predictions when we use ΔH_f (298 K) for $HO_2 = 0.499$ kcal/mol, as was used by Holgate and Tester (1993, 1994b) for their H_2 and CO models. With this lower ΔH_f (298 K) for HO_2, the model has gone from overpredicting the methane conversion to giving a very good representation of the experimental data. As noted earlier, however, this low value for ΔH_f (298 K) for HO_2 does not appear to be consistent with most other recent values. Finally, the triangles show the prediction of the model with the three adjusted preexponential factors. Again, very good agreement with experiments is obtained, but without sacrificing the thermodynamic integrity of the model.
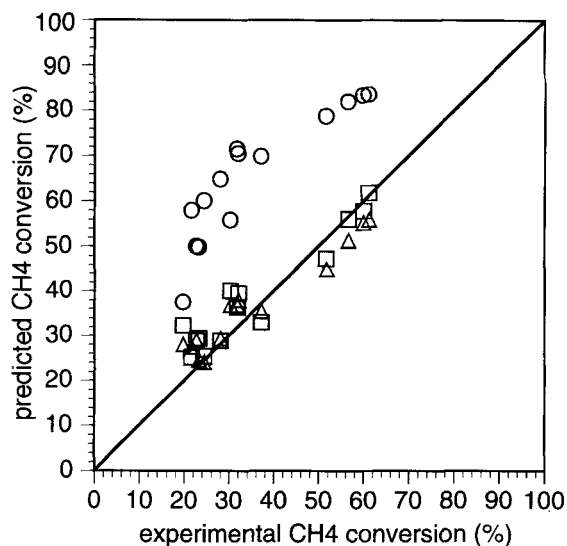
Figure 11. Comparison of predicted and experimental (Webley and Tester, 1991) methane conversions.

The circles show the predictions of the original model; the triangles show the predictions of the model with the three adjusted preexponential factors; and the squares show the predictions of the model with the JANAF HO_2 heat of formation.

Summary and Conclusions

1. Detailed chemical kinetics models based on combustion kinetics but extrapolated to high pressure can give good predictions of the kinetics reported for the SCWO of methane and hydrogen. The SCWO kinetics for methanol and carbon monoxide were predicted less accurately. Agreement between model and experimental results for all four fuels is best at high temperatures where the SCWO reaction environment can be approximated as an ideal gas.

2. Quantitative agreement can be obtained for the SCWO of methane by adjusting the preexponential factors for a few reactions within their stated uncertainties.

3. HO_2 is an important free radical in SCWO kinetics. The rate constants for reactions involving HO_2 and the thermochemical data for HO_2 must be known with better precision to reduce the uncertainty in predictive detailed chemical kinetics models for SCWO.

4. A sensitivity analysis showed that fewer than 20 elementary reactions largely control the SCWO kinetics for the disappearance of methane, methanol, CO, and hydrogen. Reducing the uncertainty in the kinetics for these reactions will have the biggest effect on reducing the uncertainty in detailed chemical kinetics models for SCWO.

5. Differences between the predictions of the detailed chemical kinetics model and experimental results for methane can be attributed to uncertainty in the kinetics and thermochemical data and to thermodynamic nonidealities. There is no need to invoke exotic supercritical fluid phenomena, such as clustering, at the conditions investigated here.

Acknowledgments

Literature Cited

Antal, Jr., M. J., A. Brittain, C. DeAlmeida, S. Ramayya, and J. C. Roy, "Heterolysis and Homolysis in Supercritical Water," *Supercritical Fluids*, T. G. Squires and M. E. Paulaitis, eds., ACS Symp. Ser., No. 329 (1987).

Basevich, V. Ya., S. M. Kogarko, and G. A. Furman, "The Reactions of Methanol with Atomic Oxygen," *Bull. Acad. Sci. USSR, Div. Chem. Sci.*, **24**, 1035 (1975).

Baulch, D. L., C. J. Cobos, R. A. Cox, C. Esser, P. Frank, Th. Just, J. A. Kerr, M. J. Pilling, J. Troe, R. W. Walker, and J. Warnatz, "Evaluated Kinetic Data for Combustion Modelling," *J. Phys. Chem. Ref. Data*, **21**, 411 (1992).

Becker, K. H., R. Kurtenbach, and P. Wiesen, "Temperature and Pressure Dependence of the Reaction $CH + H_2$," *J. Phys. Chem.*, **95**, 2390 (1991).

Benson, S. W., *Thermochemical Kinetics*, Wiley, New York (1976).

Bohland, T., S. Dobe, F. Temps, and H. Gg. Wagner, "Kinetics of the Reactions Between $CH_2(X^3B_1)$-Radicals and Saturated Hydrocarbons in the Temperature Range 296 K $\leq T \leq$ 707 K," *Ber. Bunsenges. Phys. Chem.*, **89**, 1110 (1985).

Chase, Jr., M. W., C. A. Davies, J. R. Downer, Jr., D. J. Frurip, R. A. McDonald, and A. N. Syverud, *JANAF Thermochemical Tables*, 3rd ed., *J. Phys. Chem. Ref. Data*, **14**, Suppl. No. 1 (1985).

Cobos, C. J., and J. Troe, "The Influence of Potential Energy Parameters on the Reaction $H + CH_3 = CH_4$," *Chem. Phys. Lett.*, **113**, 419 (1985).

Cochran, H. D., P. T. Cummings, and S. Karaborni, "Solvation in Supercritical Water," *Fluid Phase Equil.*, **71**, 1 (1992).

Connolly, J. F., "Solubility of Hydrocarbons in Water Near the Critical Solution Temperature," *Chem. Eng. Data*, **11**, 13 (1966).

Crain, N., S. Tebbal, X. Li, and E. F. Gloyna, "Kinetics and Reaction Pathways of Pyridine Oxidation in Supercritical Water," *Ind. Eng. Chem. Res.*, **32**, 2259 (1993).

Dean, A. J., and R. K. Hanson, "CH and C-atom Time Histories in Dilute Hydrocarbon Pyrolysis: Measurements and Kinetic Calculations," *Int. J. Chem. Kinet.*, **24**, 517 (1992).

Dean, A. M., and P. R. Westmoreland, "Biomolecular QRRK Analysis of Methyl Radical Reactions," *Int. J. Chem. Kinet.*, **19**, 207 (1987).

Dean, A. M., and G. B. Kistiakowsky, "Oxidation of Carbon Monoxide/Methane Mixtures in Shock Waves," *J. Chem. Phys.*, **54**, 1718 (1970).

Dombrowsky, Ch., and H. Gg. Wagner, "Investigation of the 3 CH_2 + O_2 Reaction in Shock Waves," *Ber. Bunsenges. Phys. Chem.*, **96**, 1048 (1992).

Frank, P., and Th. Just, "High Temperature Kinetics of Ethylene-Oxygen Reaction," *Symp. Int. Shock Tubes Proc.*, **14**, 706 (1984).

Gilbert, R. G., K. Luther, and J. Troe, "Theory of Unimolecular Reactions in the Fall-Off Range," *Ber. Bunsenges. Phys. Chem.*, **87**, 169 (1983).

Glarborg, P., J. A. Miller, and R. J. Kee, "Kinetic Modeling and Sensitivity Analysis of Nitrogen Oxide Formation in Well-Stirred Reactors," *Comb. Flame*, **65**, 177 (1986).

Gopalan, S., and P. E. Savage, "A Reaction Network Model for Phenol Oxidation in Supercritical Water," *AIChE J.*, **41**, 1864 (1995).

Greenhill, P. G., B. V. O'Grady, and R. G. Gilbert, "Theoretical Prediction of CH_3O and CH_2OH Gas Phase Decomposition Rate Coefficients," *Aust. J. Chem.*, **39**, 1929 (1986).

Hidaka, Y., T. Oki, and H. Kawano, "Thermal Decomposition of Methanol in Shock Waves," *J. Phys. Chem.*, **93**, 7134 (1989).

Hippler, H., J. Troe, and J. Willner, "Shock Wave Study of the Reaction $HO_2 + HO_2 \rightarrow H_2O_2 + O_2$: Confirmation of a Rate Constant Minimum Near 700 K," *J. Chem. Phys.*, **93**, 1755 (1990).

Holgate, H. R., and J. W. Tester, "Fundamental Kinetics and Mechanisms of Hydrogen Oxidation in Supercritical Water," *Combust. Sci. Tech.*, **88**, 369 (1993).

Holgate, H. R., P. A. Webley, J. W. Tester, and R. K. Helling, "Carbon Monoxide Oxidation in Supercritical Water: The Ef-

fects of Heat Transfer and the Water-Gas Shift Reaction on Observed Kinetics," *Energy & Fuels*, 6, 586 (1992).

Holgate, H. R., and J. W. Tester, "Oxidation of Hydrogen and Carbon Monoxide in Sub- and Supercritical Water: Reaction Kinetics, Pathways, and Water-Density Effects 1. Experimental Results," *J. Phys. Chem.*, 98, 800 (1994a).

Holgate, H. R., and J. W. Tester, "Oxidation of Hydrogen and Carbon Monoxide in Sub- and Supercritical Water: Reaction Kinetics, Pathways, and Water-Density Effects 2. Elementary Reaction Modeling," *J. Phys. Chem.*, 98, 810 (1994b).

Kee, R. J., F. M. Rupley, and J. A. Miller, "The CHEMKIN Thermodynamic Data Base," Sandia National Laboratories, SAND87-8215 (1991).

Kee, R. J., F. M. Rupley, and J. A. Miller, "CHEMKIN II: A FORTRAN Chemical Kinetics Package for the Analysis of Gas-Phase Chemical Kinetics," Sandia National Laboratories, SAND89-8009 (1990).

Larson, C. W., P. H. Stewart, and D. M. Golden, "Pressure and Temperature Dependence of Reactions Proceeding Via a Bound Complex: An Approach for Combustion and Atmospheric Chemistry Modelers. Application to $HO + CO \rightarrow [HOCO] \rightarrow H + CO_2$," *Int. J. Chem. Kinet.*, 20, 27 (1988a).

Larson, C. W., P. H. Stewart, and D. M. Golden, "Errata," *Int. J. Chem. Kinet.*, 20, 493 (1988b).

Lee, D.-S., and E. F. Gloyna, "Hydrolysis and Oxidation of Acetamide in Supercritical Water," *Env. Sci. Tech.*, 26, 1587 (1992).

Li, R., P. E. Savage, and D. Szmukler, "2-Chlorophenol Oxidation in Supercritical Water: Global Kinetics and Reaction Products," *AIChE J.*, 39, 178 (1993).

Li, R., T. D. Thornton, and P. E. Savage, "Kinetics of CO_2 Formation from the Oxidation of Phenols in Supercritical Water," *Env. Sci. Tech.*, 26, 2388 (1992).

Lichtin, D. A., M. C. Berman, and M. C. Lin, "Kinetic Studies of Initiated Reactions of CH and CN Radicals," *Bull. Soc. Chim. Belg.*, 92, 656 (1983).

Lutz, A. E., R. J. Kee, and J. A. Miller, "SENKIN: A FORTRAN Program for Predicting Homogeneous Gas Phase Chemical Kinetics with Sensitivity Analysis," Sandia National Laboratories, SAND87-8248 (1991).

Mallard, W. G., F. Westley, J. T. Herron, R. F. Hampson, and D. H. Frizzell, *NIST Chemical Kinetics Database: Version 5.0*, National Institute of Standards and Technology, Gaithersburg, MD (1993).

Marshall, William L., and E. U. Franck, "Ion Product of Water Substance, 0–1000°C, 1–10,000 bar New International Formulation and Its Background," *J. Phys. Chem. Ref. Data*, 10, 295 (1981).

Modell, M., in *Standard Handbook of Hazardous Waste Treatment and Disposal*, Sec. 8.11, H. M. Freeman, ed., McGraw-Hill, New York (1989).

Pray, H. A., C. E. Schweickert, and B. H. Minnich, "Solubility of Hydrogen, Oxygen, Nitrogen, and Helium in Water," *Ind. Eng. Chem.*, 44, 1146 (1952).

Ritter, E. R., and J. W. Bozzelli, "THERM: Thermodynamic Property Estimation for Gas Phase Radicals and Molecules," *Int. J. Chem. Kinet.*, 23, 767 (1991).

Rofer, C. K., and G. E. Streit, "Kinetics and Mechanisms of Methane Oxidation in Supercritical Water," Los Alamos National Laboratory Report, LA-11439-MS (1988).

Rofer, C. K., and G. E. Streit, "Phase II Final Report: Oxidation of Hydrocarbons and Organics in Supercritical Water," Los Alamos National Laboratory Report, LA-11700-MS (1989).

Sander, S. P., and R. T. Watson, "Kinetics Studies of the Reactions of CH_3O_2 with NO, NO_2 and CH_3O_2 at 298 K," *J. Phys. Chem.*, 84, 1664 (1980).

Savage, P. E., and M. A. Smith, "Kinetics of Acetic Acid Oxidation in Supercritical Water," *Env. Sci. Tech.*, 29, 216 (1995).

Schmitt, R. G., P. B. Butler, and N. Bergan-French, "CHEMKIN Real Gas: A FORTRAN Package for Analysis of Thermodynamic Properties and Chemical Kinetics in Nonideal Systems," University of Iowa, UIME PBB 93-006, Iowa City (1994).

Senkan, S. M., "Detailed Chemical Kinetic Modeling: Chemical Reaction Engineering of the Future," *Adv. Chem. Eng.*, Vol. 18, Academic Press, New York, p. 95 (1992).

Slemr, F., and P. Warneck, "Kinetics of the Reaction of Atomic Hydrogen with Methyl/Hydroperoxide," *Int. J. Chem. Kinet.*, 9, 267 (1977).

Steinfeld, J. I., J. S. Francisco, and W. L. Hase, *Chemical Kinetics and Dynamics*, Prentice-Hall, Englewood Cliffs, NJ (1989).

Stewart, P. H., C. W. Larson, and D. Golden, "Pressure and Temperature Dependence of Reactions Proceeding via a Boundary Complex: 2. Application to $2CH_3 \rightarrow C_2H_5 + H$," *Comb. Flame*, 75, 25 (1989).

Tester, J. W., P. A. Webley, and H. R. Holgate, "Revised Global Kinetics Measurements of Methanol Oxidation in Supercritical Water," *Ind. Eng. Chem. Res.*, 32, 236 (1993).

Thomason, T. B., and M. Modell, "Supercritical Water Destruction of Aqueous Wastes," *Haz. Waste*, 1, 453 (1984).

Thornton, T. D., and P. E. Savage, "Phenol Oxidation Pathways in Supercritical Water," *Ind. Eng. Chem. Res.*, 31, 2451 (1992a).

Thornton, T. D., and P. E. Savage, "Kinetics of Phenol Oxidation in Supercritical Water," *AIChE J.*, 38, 321 (1992b).

Thornton, T. D., D. E. LaDue, and P. E. Savage, "Phenol Oxidation in Supercritical Water: Formation of Dibenzofuran, Dibenzo-p-dioxin, and Related Compounds," *Env. Sci. Tech.*, 25, 1507 (1991).

Troe, J., "Theory of Thermal Unimolecular Reactions at Low Pressures: II. Strong Collision Rate Constants. Applications," *J. Chem. Phys.*, 66, 4745 (1977).

Tsang, W., "Chemical Kinetic Data Base for Combustion Chemistry. Part 2. Methanol," *J. Phys. Chem. Ref. Data*, 16, 471 (1987).

Tsang, W., and R. F. Hampson, "Chemical Kinetic Data Base for Combustion Chemistry. Part 1. Methane and Related Compounds," *J. Phys. Chem. Ref. Data*, 15, 1087 (1986).

Tsuboi, T., and K. Hashimoto, "Shock Tube Study on Homogeneous Thermal Oxidation of Methanol," *Comb. Flame*, 42, 61 (1981).

Wallington, T. J., P. Dagaut, and M. J. Kurylo, "Ultraviolet Absorption Cross Sections and Reaction Kinetics and Mechanisms for Peroxy Radicals in the Gas Phase," *Chem. Rev.*, 92, 667 (1992).

Warnatz, J., "Rate Coefficients in the C/H/O System," *Combustion Chemistry*, W. C. Gardiner, Jr., ed., Springer-Verlag, New York, p. 197 (1984).

Webley, P. A., H. R. Holgate, D. M. Stevenson, and J. W. Tester, "Oxidation Kinetics of Model Compounds of Metabolic Waste in Supercritical Water," *SAE Tech.*, Paper 901333 (1990).

Webley, P. A., and J. W. Tester, "Fundamental Kinetics of Methane Oxidation in Supercritical Water," *Energy & Fuels*, 5, 411 (1991).

Webley, P. A., "Fundamental Oxidation Kinetics of Simple Compounds in Supercritical Water," PhD Thesis, Massachusetts Institute of Technology, Cambridge (1989).

Yang, H. H., and C. A. Eckert, "Homogeneous Catalysis in the Oxidation of p-Chlorophenol in Supercritical Water," *Ind. Eng. Chem. Res.*, 27, 2009 (1988).

Zabarnick, S., J. W. Fleming, and M. C. Lin, "Temperature Dependence of CH Radical Reactions with H_2O and CH_2O," *Symp. (Int.) Combust. Proc.*, 21, 713 (1988).